

**Supplemental information**

**PD-1<sup>high</sup>CXCR5<sup>-</sup>CD4<sup>+</sup> peripheral helper T cells**

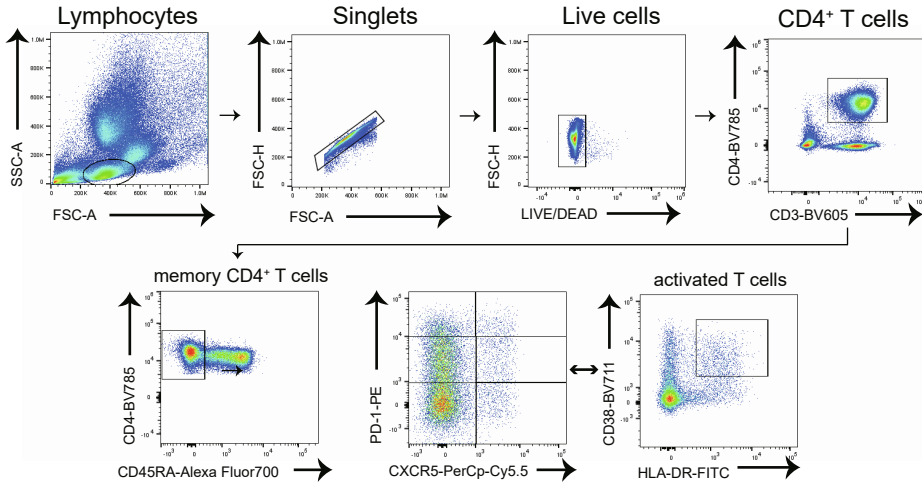
**promote CXCR3<sup>+</sup> plasmablasts**

**in human acute viral infection**

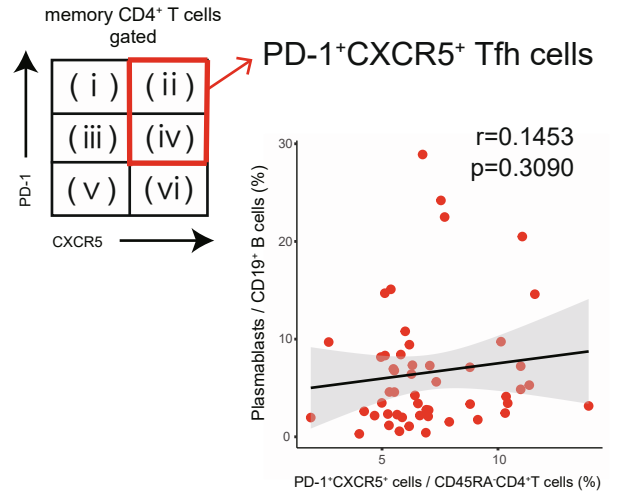
**Hiromitsu Asashima, Subhasis Mohanty, Michela Comi, William E. Ruff, Kenneth B. Hoehn, Patrick Wong, Jon Klein, Carolina Lucas, Inessa Cohen, Sarah Coffey, Nikhil Lele, Leissa Greta, Khadir Raddassi, Omkar Chaudhary, Avraham Unterman, Brinda Emu, Steven H. Kleinstein, Ruth R. Montgomery, Akiko Iwasaki, Charles S. Dela Cruz, Naftali Kaminski, Albert C. Shaw, David A. Hafler, and Tomokazu S. Sumida**

# Supplemental Figure 1

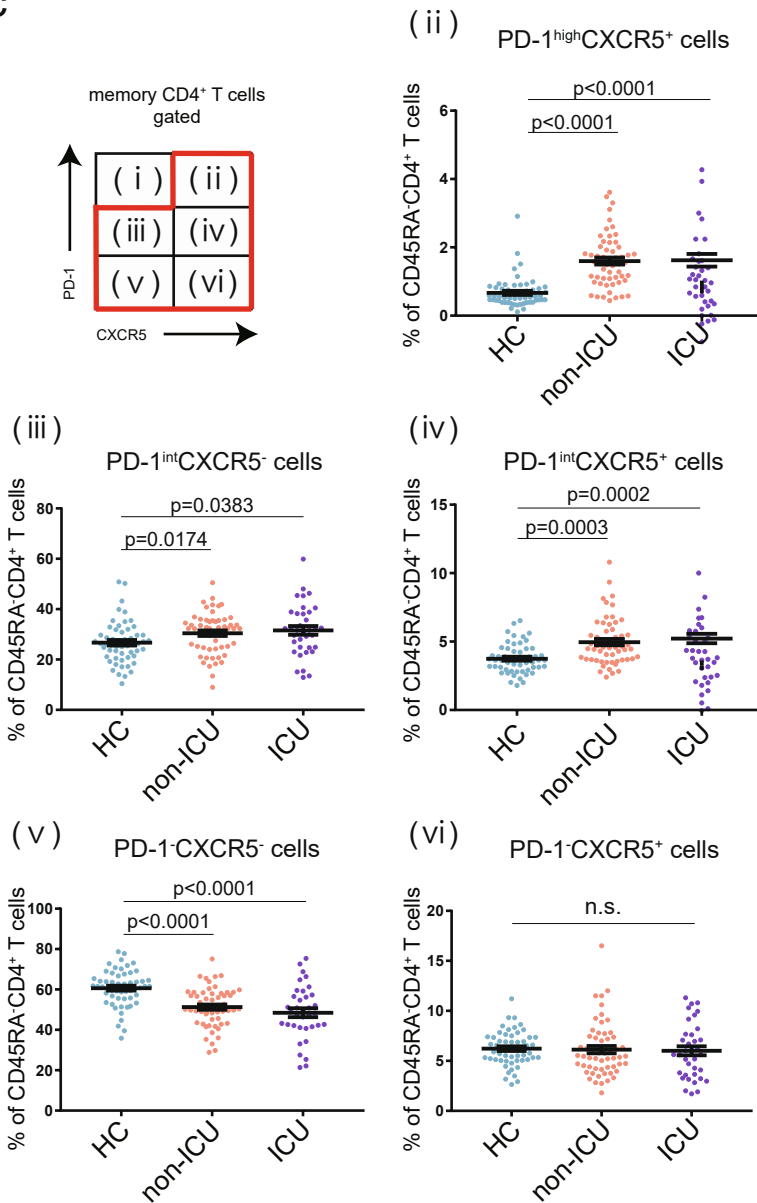
**a**



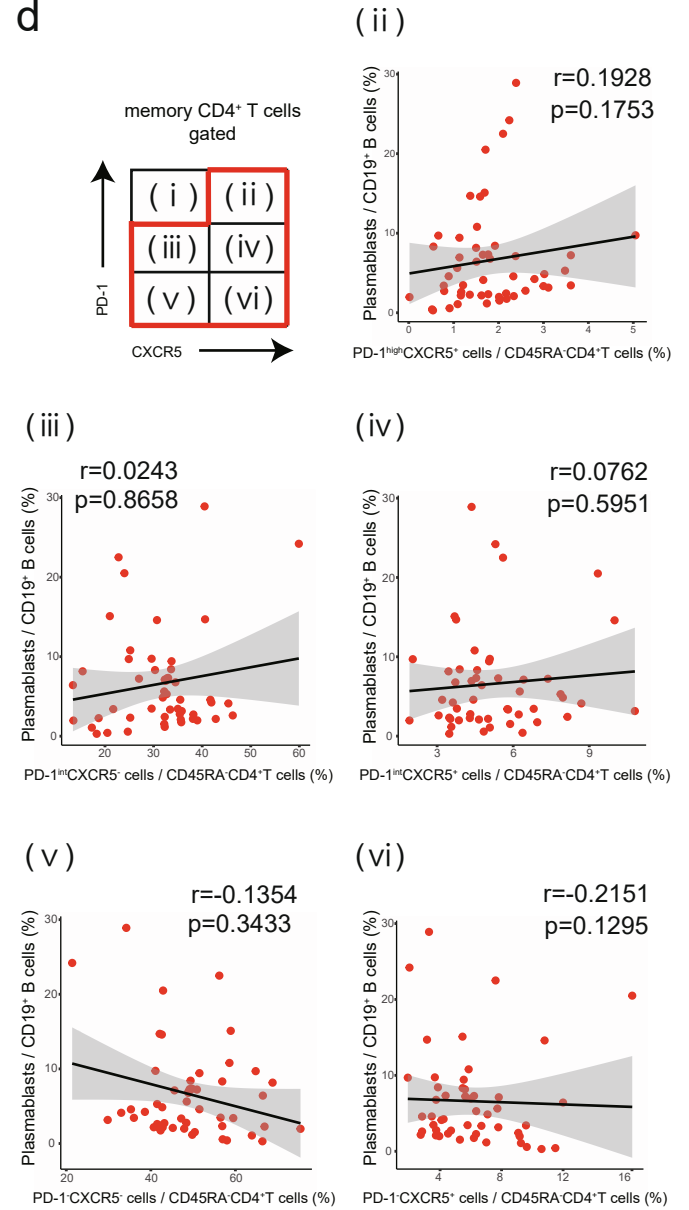
**b**



**c**



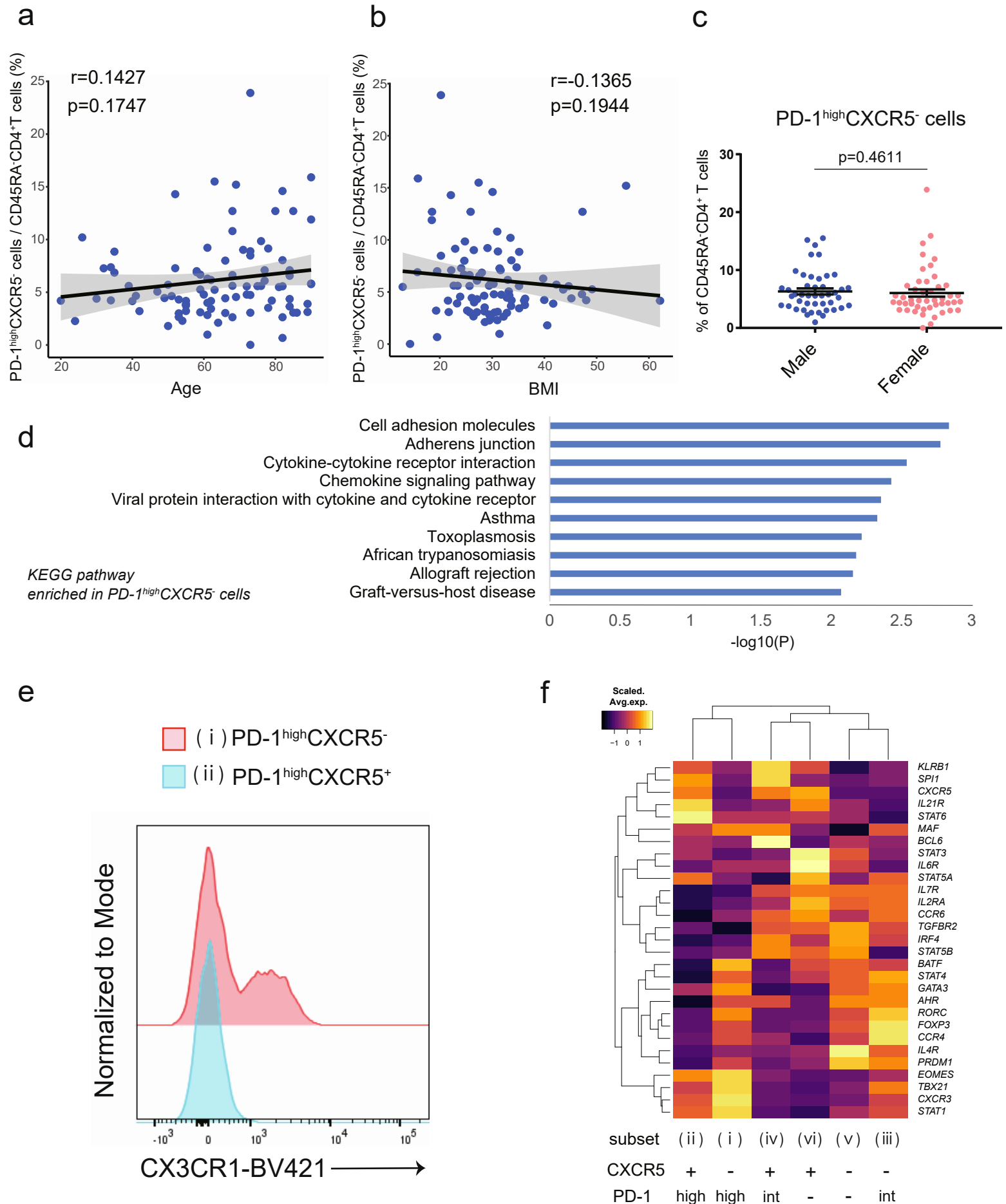
**d**



**Supplemental Figure 1 The characteristics of each T cell subset.** Related to Figure 1.

**a**, Gating strategy to identify each T cell subset in PBMCs. Six subsets were detected based on the expression levels of PD-1 and CXCR5, and activated T cells were defined as HLA-DR<sup>+</sup>CD38<sup>+</sup> T cells. **b**, Correlation between PD-1<sup>+</sup>CXCR5<sup>+</sup> Tfh cells (both PD-1<sup>high</sup>CXCR5<sup>+</sup> and PD-1<sup>int</sup>CXCR5<sup>+</sup> Tfh cells) and plasmablasts (percentage of CD19<sup>+</sup> B cells) in COVID-19 patients (both non-ICU and ICU, n=51). **c**, The proportion of each T cell subset among healthcare workers (HC) (n=55), non-ICU COVID-19 patients (non-ICU) (n=56), and ICU patients (ICU) (n=36). One-way ANOVA with Dunn's multiple comparisons tests were evaluated. n.s. = no significance among each group. Data are represented as mean ± SEM. **d**, Correlation between each T cell subset (percentage of CD3<sup>+</sup>CD4<sup>+</sup>CD45RA<sup>-</sup> memory T cells) and plasmablasts (percentage of CD19<sup>+</sup> B cells) in COVID-19 patients (both non-ICU and ICU, n=51). Linear regression is shown with 95% confidence interval (gray area). Correlation statistics is two-tailed Spearman's rank correlation test.

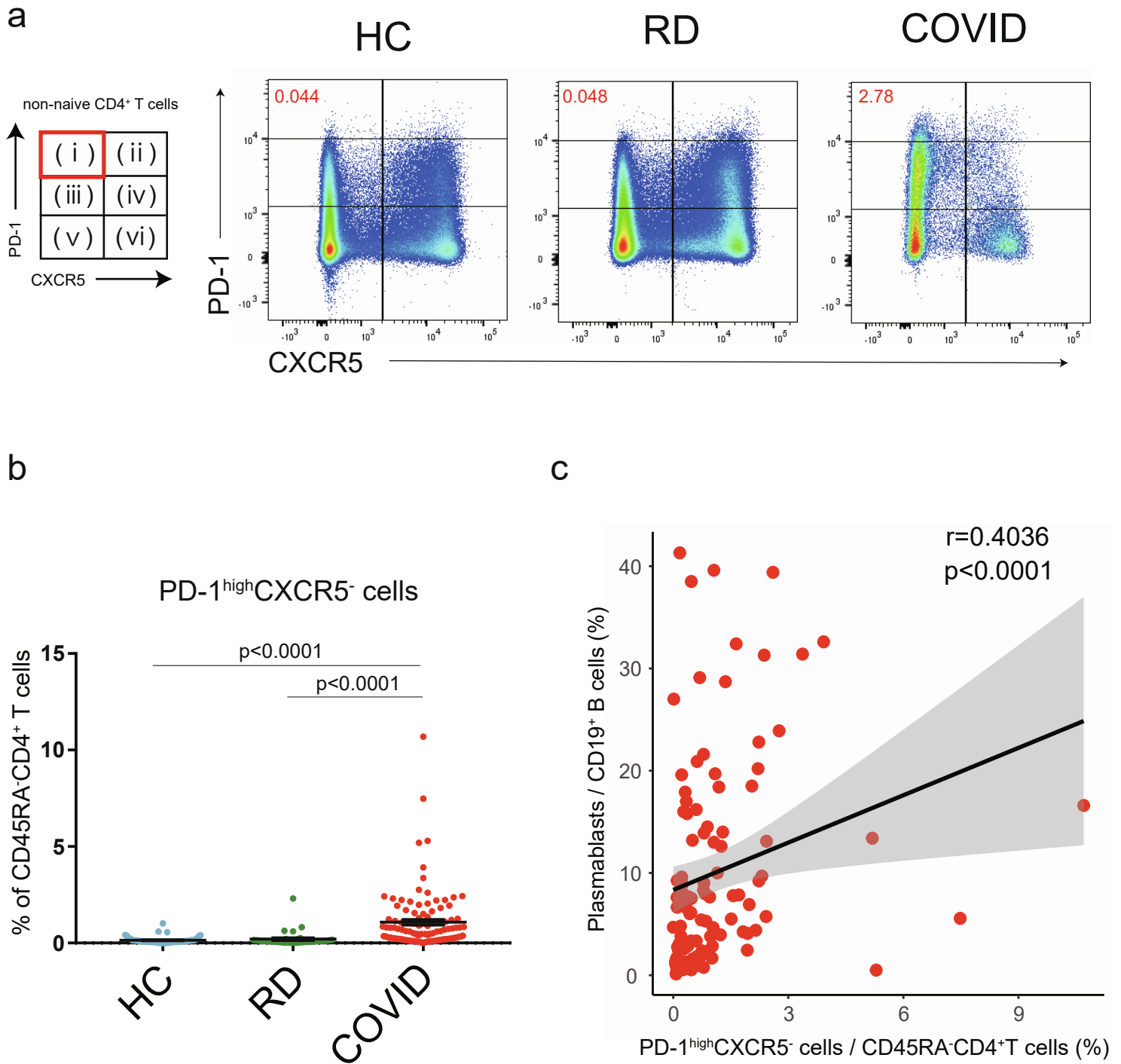
## Supplemental Figure 2



### Supplemental Figure 2 The characteristics of PD-1<sup>high</sup>CXCR5<sup>-</sup> Tph cells. Related to Figure 1.

**a-b**, Correlation between the proportion of PD-1<sup>high</sup>CXCR5<sup>-</sup> Tph cells (percentage of CD3<sup>+</sup>CD4<sup>+</sup>CD45RA<sup>-</sup> memory T cells) and each clinical background in COVID-19 patients (both non-ICU and ICU, n=92) (**a**, age; **b**, BMI). Linear regression is shown with 95% confidence interval (gray area). Correlation statistics by two-tailed Spearman' s rank correlation test (**a**, **b**). **c**, The proportion of PD-1<sup>high</sup>CXCR5<sup>-</sup> Tph cells between male (n=45) and female (n=47) COVID-19 patients were evaluated by two-tailed unpaired Student' s t-test. Data are represented as mean  $\pm$  SEM. **d**, Analysis of pathways using EnrichR for upregulated genes in PD-1<sup>high</sup>CXCR5<sup>-</sup> Tph cells compared with PD-1<sup>high</sup>CXCR5<sup>+</sup> Tfh cells. **e**, Representative flow data of CX3CR1 expression on PD-1<sup>high</sup>CXCR5<sup>-</sup> Tph cells compared with PD-1<sup>high</sup>CXCR5<sup>+</sup> Tfh cells. **f**, Heatmap of T cell lineage genes among six subsets of memory CD4<sup>+</sup> T cells.

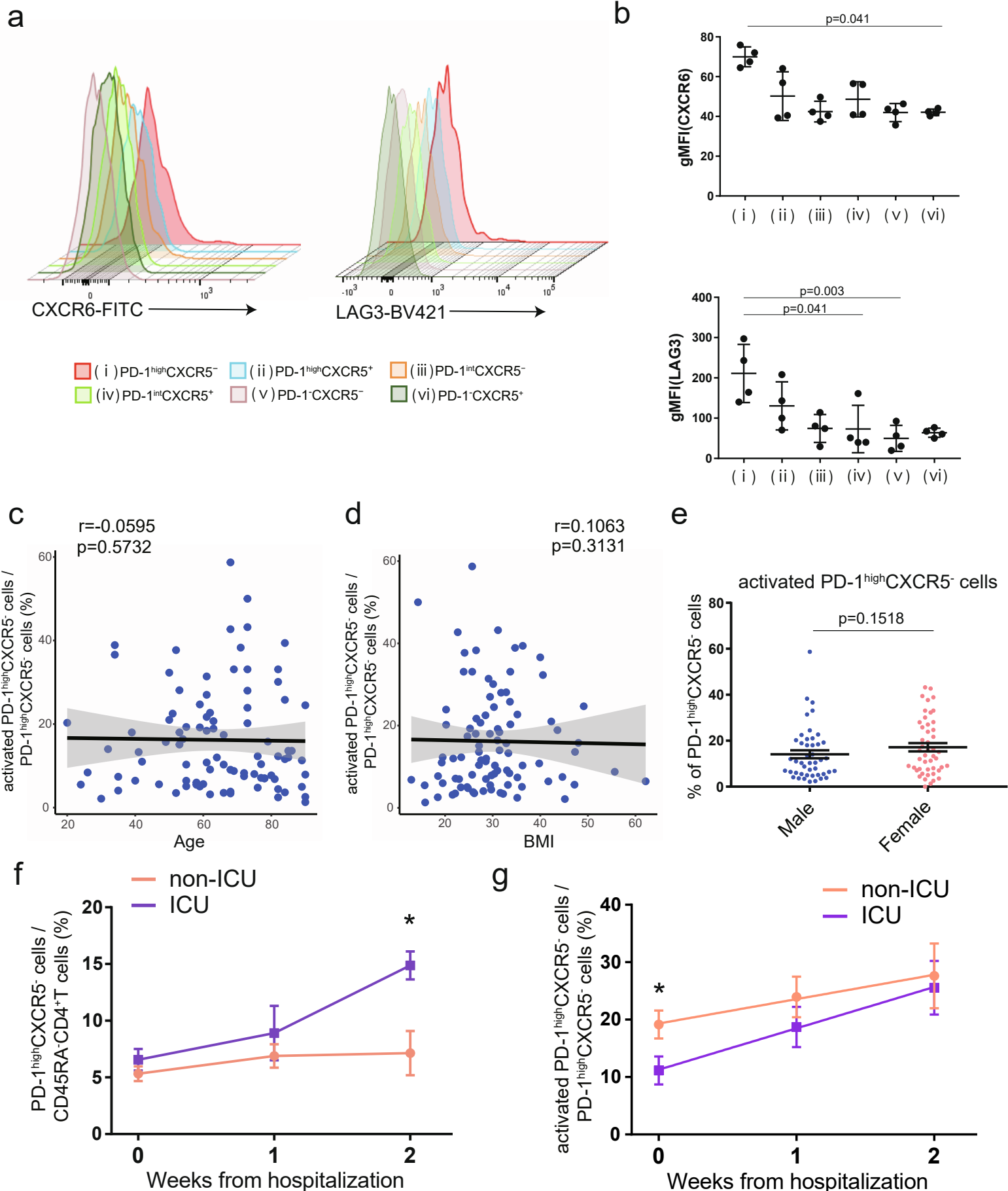
# Supplemental Figure 3



## Supplemental Figure 3 PD-1<sup>high</sup>CXCR5<sup>-</sup> Tph cells from another COVID-19 dataset. Related to Figure 1.

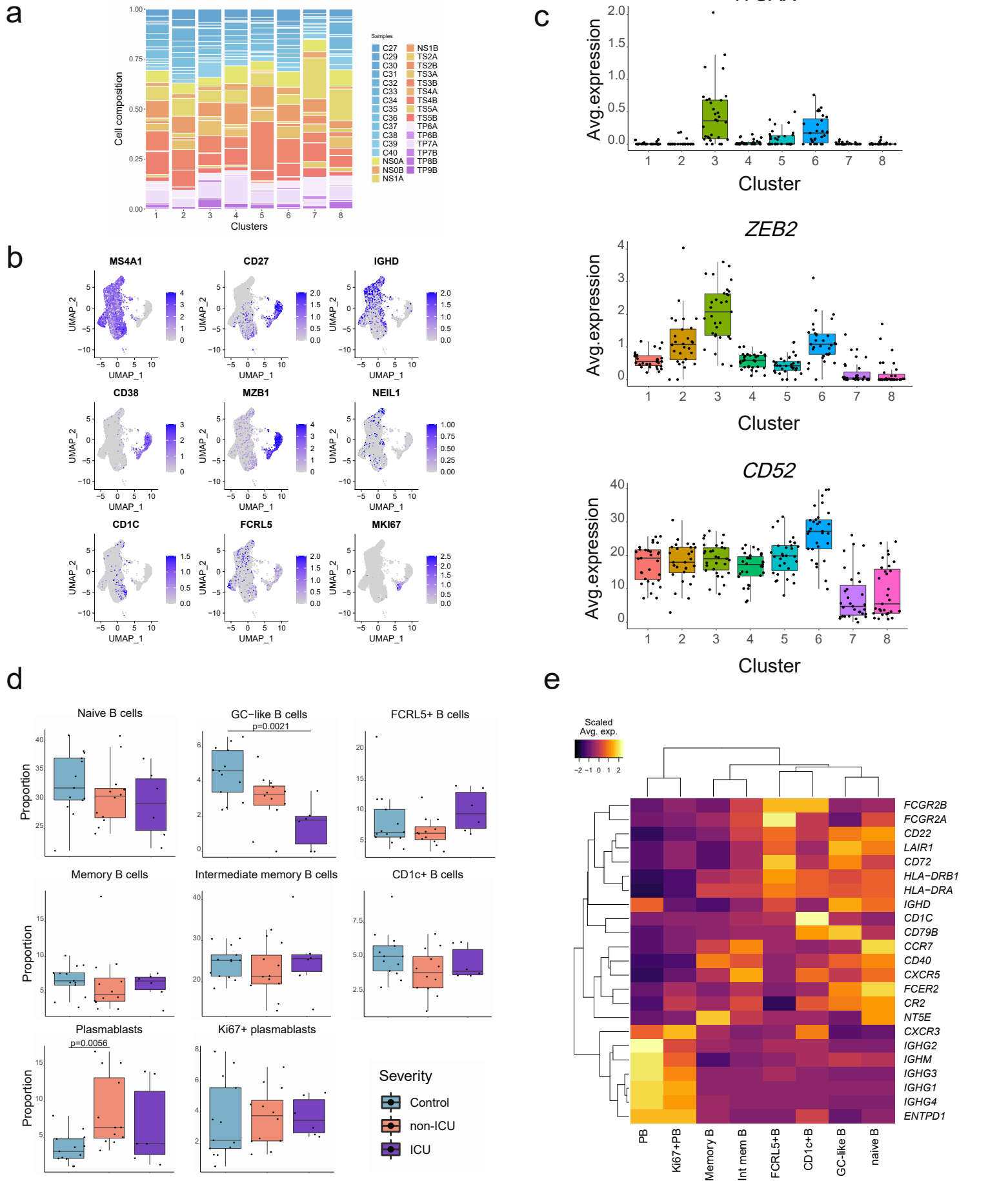
Deposited flow cytometry data from another study<sup>[S1]</sup> were analyzed for validation of the characteristics of PD-1<sup>high</sup>CXCR5<sup>-</sup> Tph cells in the acute phase of COVID-19 patients. **a**, Representative flow data of PD-1<sup>high</sup>CXCR5<sup>-</sup> Tph cells in healthy donors (HC), recovered donors from COVID-19 (RD), and hospitalized COVID-19 patients (COVID). **b**, The proportion of PD-1<sup>high</sup>CXCR5<sup>-</sup> Tph cells among HC (n=56), RD (n=36), and COVID (n=109; all at baseline samples) groups. One-way ANOVA with Dunn's multiple comparisons tests were performed to evaluate differences. **c**, Correlation between PD-1<sup>high</sup>CXCR5<sup>-</sup> Tph cells (percentage of CD3<sup>+</sup>CD4<sup>+</sup>CD45RA<sup>-</sup> non-naive T cells) and plasmablasts (percentage of CD19<sup>+</sup> B cells) in COVID-19 patients (n=109). Linear regression is shown with 95% confidence interval (gray area). Correlation statistics is two-tailed Spearman's rank correlation test.

Supplemental Figure 4



**Supplemental Figure 4** The characteristics of HLA-DR<sup>+</sup>CD38<sup>+</sup> activated PD-1<sup>high</sup>CXCR5<sup>-</sup> Tph cells. Related to Figure 2. **a**, Representative flow data of CXCR6 and LAG3 on each T cell subset. **b**, LAG3 (left) and CXCR6 (right) gMFI of each T cell subset were evaluated (n=4, COVID-19 patients). One-way ANOVA with Dunn's multiple comparisons tests were evaluated. **c-d**, Correlation between the proportion of activated HLA-DR<sup>+</sup>CD38<sup>+</sup>PD-1<sup>high</sup>CXCR5<sup>-</sup> Tph cells (percentage of PD-1<sup>high</sup>CXCR5<sup>-</sup> Tph cells) and each clinical background in COVID-19 patients (both non-ICU and ICU, n=92)(**c**, age; **d**, BMI). Linear regression is shown with 95% confidence interval (gray area). Correlation statistics is two-tailed Spearman's rank correlation test (**c**, **d**). **e**, The proportion of activated HLA-DR<sup>+</sup>CD38<sup>+</sup>PD-1<sup>high</sup>CXCR5<sup>-</sup> Tph cells between male (n=45) and female (n=47) COVID-19 patients were evaluated by two-tailed unpaired Student's t-test. **f-g**, Longitudinal frequencies of PD-1<sup>high</sup>CXCR5<sup>-</sup> Tph cells (**f**) and activated PD-1<sup>high</sup>CXCR5<sup>-</sup> Tph cells (**g**) after hospitalization. Only the samples which could follow blood collection (hospitalization, week1 of day1-7, week2 of day8-14) were analyzed (non-ICU n=23, ICU n=16). At each time point, Two-tailed unpaired Student's t-test were performed (\*p<0.05). Data are represented as mean ± SEM.

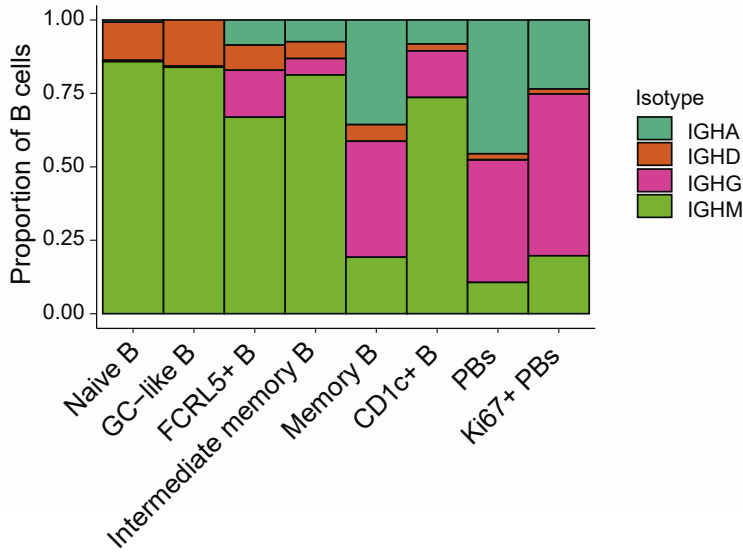
# Supplemental Figure 5



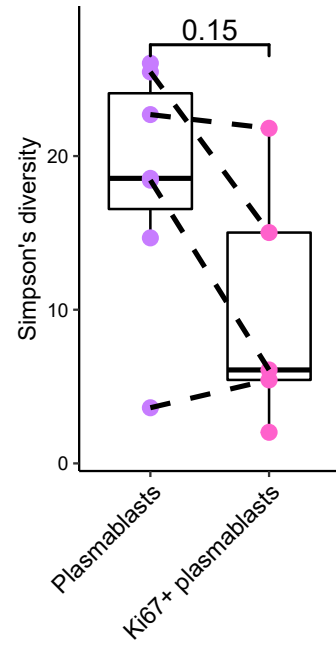
**Supplemental Figure 5 The characteristics of each B cell subset in scRNA-seq dataset.** Related to Figure 3. **a**, Bar plot showing cell compositions of each cluster by samples. C; control, NS; tocilizumab non-treated stable (non-ICU) patients, TS; tocilizumab-treated stable (non-ICU) patients, TP; tocilizumab-treated progressive (ICU) patients. **b**, Canonical cell markers for cluster delineation. Data are colored according to expression levels. **c**, Box plot showing other canonical markers. The median is marked by a horizontal line with whiskers extending to the farthest point within a maximum of 1.5 x interquartile range. Each dot corresponds to each sample. **d**, Comparison of cell counts (percentage of total B cells) among each group (one-way ANOVA with Dunnett' s multiple comparisons test). Each dot corresponds to each sample, and One-way ANOVA with Dunn' s multiple comparisons test was performed. **e**, Heatmap of gene expressions related to B cell functions<sup>[S2]</sup> in each cluster. All the samples are evaluated.

# Supplemental Figure 6

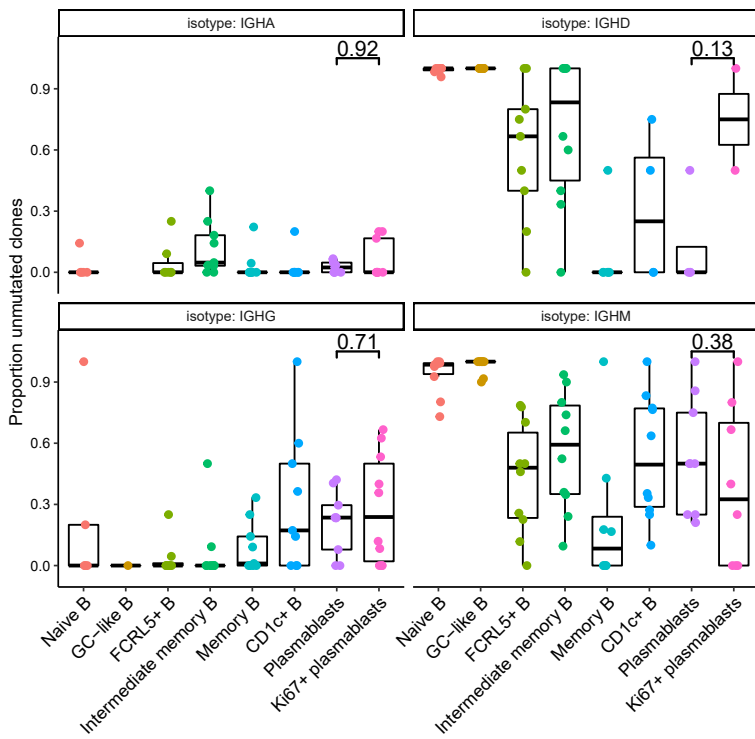
**a**



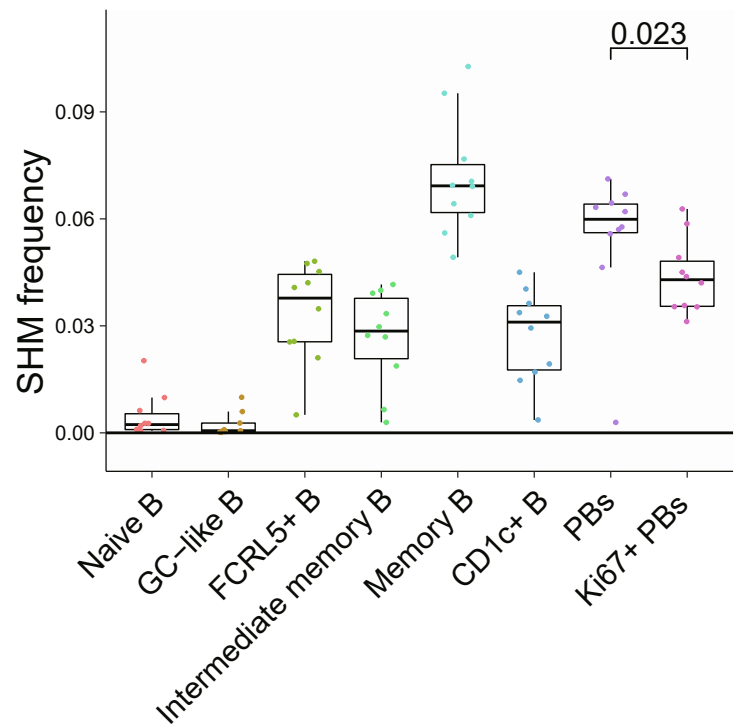
**b**



**c**



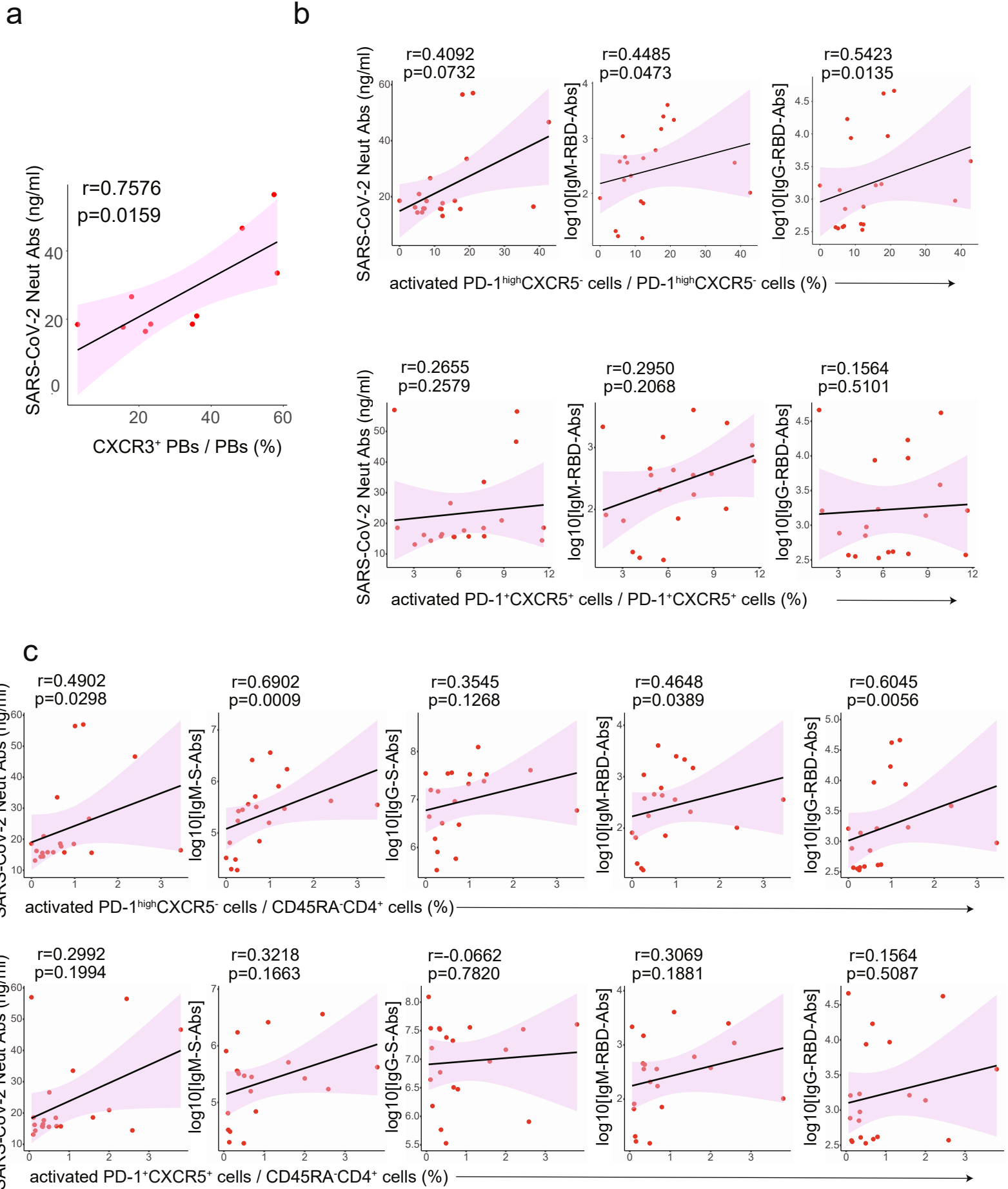
**d**



**Supplemental Figure 6 BCR repertoires in scRNA-seq dataset.** Related to Figure 3.

**a**, Fractional abundance of IGHA (dark green), IGHD (orange), IGHG (pink), and IGHM (light green) cells in each cluster. PBs denote plasmablasts. **b**, Simpson's diversity of B cell clones within each plasmablast cluster. Each dot corresponds to a patient (combined early and late samples), and dots from the same patient are connected with dotted lines. **c**, Proportion of unmutated clones within each cell type cluster based on immunoglobulin isotypes. Each dot corresponds to a patient, and a Wilcoxon test p value is reported above plasmablast clusters. **d**, Frequency of somatic hypermutation (SHM) in each cluster. Each dot denotes a patient (combined early and late samples, n=10). A Wilcoxon test was evaluated, and p value is reported above plasmablast clusters.

Supplemental Figure 7



**Supplemental Figure 7 The relationship between each subset and anti-SARS-CoV-2 antibodies.** Related to Figure 3. **a**, Correlation between CXCR3<sup>+</sup> plasmablasts (percentage of plasmablasts) and SARS-CoV-2 neutralizing antibodies (ng/ml) in COVID-19 patients (n=10, all samples are within 14 days after first symptoms). Linear regression is shown with 95% confidence interval (pink area). Correlation statistics is two-tailed Spearman' s rank correlation test. **b**, Correlation between HLA-DR<sup>+</sup>CD38<sup>+</sup> activated PD-1<sup>high</sup>CXCR5<sup>-</sup> Tph cells (percentage of Tph cells) or HLA-DR<sup>+</sup>CD38<sup>+</sup> activated PD-1<sup>+</sup>CXCR5<sup>+</sup> Tfh cells (percentage of Tfh cells) and anti-SARS-CoV-2 antibodies (log10 scaled) or neutralizing antibodies (ng/ml) in COVID-19 patients (n=20). **c**, Correlation between HLA-DR<sup>+</sup>CD38<sup>+</sup> activated PD-1<sup>high</sup>CXCR5<sup>-</sup> Tph cells or PD-1<sup>+</sup>CXCR5<sup>+</sup> Tfh cells (percentage of memory CD4<sup>+</sup> T cells) and anti-SARS-CoV-2 antibodies (log10 scaled) or neutralizing antibodies (ng/ml) in COVID-19 patients (n=20). Linear regression is shown with 95% confidence interval (pink area). Correlation statistics is two-tailed Spearman' s rank correlation test.



## Supplemental References

- S1. Mathew, D., Giles, J.R., Baxter, A.E., Greenplate, A.R., Wu, J.E., Alanio, C., Oldridge, D.A., Kuri-Cervantes, L., Pampena, M.B., D'Andrea, K., et al. (2020). Deep immune profiling of COVID-19 patients reveals patient heterogeneity and distinct immunotypes with implications for therapeutic interventions. *Science*. 369, eabc8511.  
<https://doi.org/10.1126/science.abc8511>.
- S2. Glass, D.R., Tsai, A.G., Oliveria, J.P., Hartmann, F.J., Kimmey, S.C., Calderon, A.A., Borges, L., Glass, M.C., Wagar, L.E., Davis, M.M., et al. (2020). An Integrated Multi-omic Single-Cell Atlas of Human B Cell Identity. *Immunity*. 53, 217-232.e5.  
<https://doi.org/10.1016/j.immuni.2020.06.013>.